

N90-20776

OPTICAL CONSTANTS OF KEROGEN FROM 0.15 TO 40 μm :
COMPARISON WITH METEORITIC ORGANICSBISHUN N. KHARE,* W.R. THOMPSON,* C. SAGAN,* E.T. ARAKAWA,** C. MEISSE,** AND
I. GILMOUR,*,***Laboratory for Planetary Studies, Cornell University, Ithaca, New York, 14853,
U.S.A.

**Oak Ridge National Laboratory, Oak Ridge, Tennessee 37831, U.S.A.

*Enrico Fermi Institute and Department of Chemistry, University of Chicago, Chicago,
IL 60637, U.S.A.**Present address: Planetary Sciences Unit, The Open University, Milton Keynes, MK7
6AA, U.K.

ABSTRACT

Kerogens are dark, complex organic materials produced on the Earth primarily by geologic processing of biologic materials, but kerogens have chemical and spectral similarities to some classes of highly processed extraterrestrial organic materials. Kerogen-like solids have been proposed as constituents of the very dark reddish surfaces of some asteroids [Gradie and Veverka, *Nature* 283, 840 (1980)] and are also spectrally similar to some carbonaceous organic residues and the Iapetus dark material [Cruikshank et al., *Icarus* 53, 90 (1983)]. Kerogen can thus serve as a useful laboratory analogue to very dark, spectrally red extraterrestrial materials; its optical constants can be used to investigate the effects of particle size, void space and mixing of bright and dark components in models of scattering by dark asteroidal, cometary, and satellite surfaces.

We report measurements of the optical constants of both Type II kerogen and of macromolecular organic residue from the Murchison carbonaceous chondrite via transmission and reflection measurements on thin films. These films, of thickness 0.2-1.3 μm , are produced by vacuum deposition of kerogen powder heated to 550-750°C onto sapphire, CaF_2 , and CsI substrates. IR spectra of the thin films show that the spectral features of the kerogen powder are retained. Apparently no substantial change in optical constants occurs upon vacuum deposition, except for the desirable loss of silicate contaminants which can be seen in the spectra of the powder.

The real part of the refractive index, n , is determined by variable incidence-angle reflectance to be 1.60 ± 0.05 from 0.4-2.0 μm wavelength. Work extending the measurement of n to longer wavelengths is in progress. The imaginary part of the refractive index, k , shows substantial structure from 0.15-40 μm . The values are accurate to $\pm 20\%$ in the UV and IR regions and to $\pm 30\%$ in the visible. We have also measured k values of organic residues from the Murchison meteorite. Comparison of the kerogen and Murchison data reveals that between 0.15 and 40 μm , Murchison has a similar structure but no bands as sharp as in kerogen, and that the k values for

Murchison are significantly higher than those of kerogen.

INTRODUCTION

Kerogens are dark, complex organic materials produced on earth from biologically derived organic material that has been incorporated into sediments where it has undergone further geological processing.^{1,2} Kerogens can be classified as either Type I, II or III depending on their H/C and O/C elemental ratios.³ These classifications reflect the origins and chemical structures of the kerogens. Type I is derived from predominantly aliphatic algal material, Type II from lipid-rich marine material, and Type III from more aromatic-rich terrestrial organic matter.⁴ Within each type, individual samples differ according to the degree of geologic processing but originate from the same type of parent material.⁵ While of biotic origin, kerogens have chemical and spectral similarities to some types of highly processed extraterrestrial organic materials. Kerogen-like solids have been proposed as constituents of the very dark reddish surfaces of some asteroids⁶ and are also similar to the Iapetus dark material.⁷ Kerogens can thus serve as useful laboratory analogues to very dark, spectrally red extraterrestrial materials. Measurements of their optical constants can be used to investigate the effect of particle size, void space, and mixing of bright and dark components in models of scattering by dark asteroids, cometary and satellite surfaces.

Here, using high-vacuum film deposition and transmission spectroscopic techniques, we study and compare the optical constants of a Type II kerogen and of organic residue from the Murchison carbonaceous chondrite. Meteorites were formed in the solar nebula, where organic material is thought to have been produced by catalytic reactions of carbon monoxide, hydrogen, and ammonia,⁸ and by ultraviolet and charged particle irradiation.⁹ Hayatsu and co-workers¹⁰ have undertaken extensive investigations of the structure of Murchison organic materials using a variety of degradation techniques. They conclude that the material is comprised of condensed aromatic and heterocyclic ring systems cross-linked by short methylene chains, ethers, sulfides, and biphenyl groups.^{10,11} These chemical structures are similar to those of kerogen. Comparison of the spectroscopic properties of the extraterrestrial abiotic Murchison organic residue and the terrestrial metamorphosed biotic material that composes kerogen provides further insight into their structural and chemical similarities and differences.

EXPERIMENTAL

(a) Sample Information

The kerogen sample is a 190 million year old Type II kerogen from the Isle of

Skye, Scotland. The extraction of kerogen from the sedimentary rocks followed the procedure used by Durand and Nicaise.¹² The meteoritic material used is a sample of "macromolecular" organic material isolated by acid-dissolution and solvent extractions from the Murchison carbonaceous chondrite; a similar procedure is used for kerogen.

(b) Film Preparation

Films of kerogen and of Murchison organic material were prepared by thermal evaporation. The experimental set-up is shown in Figure 1.

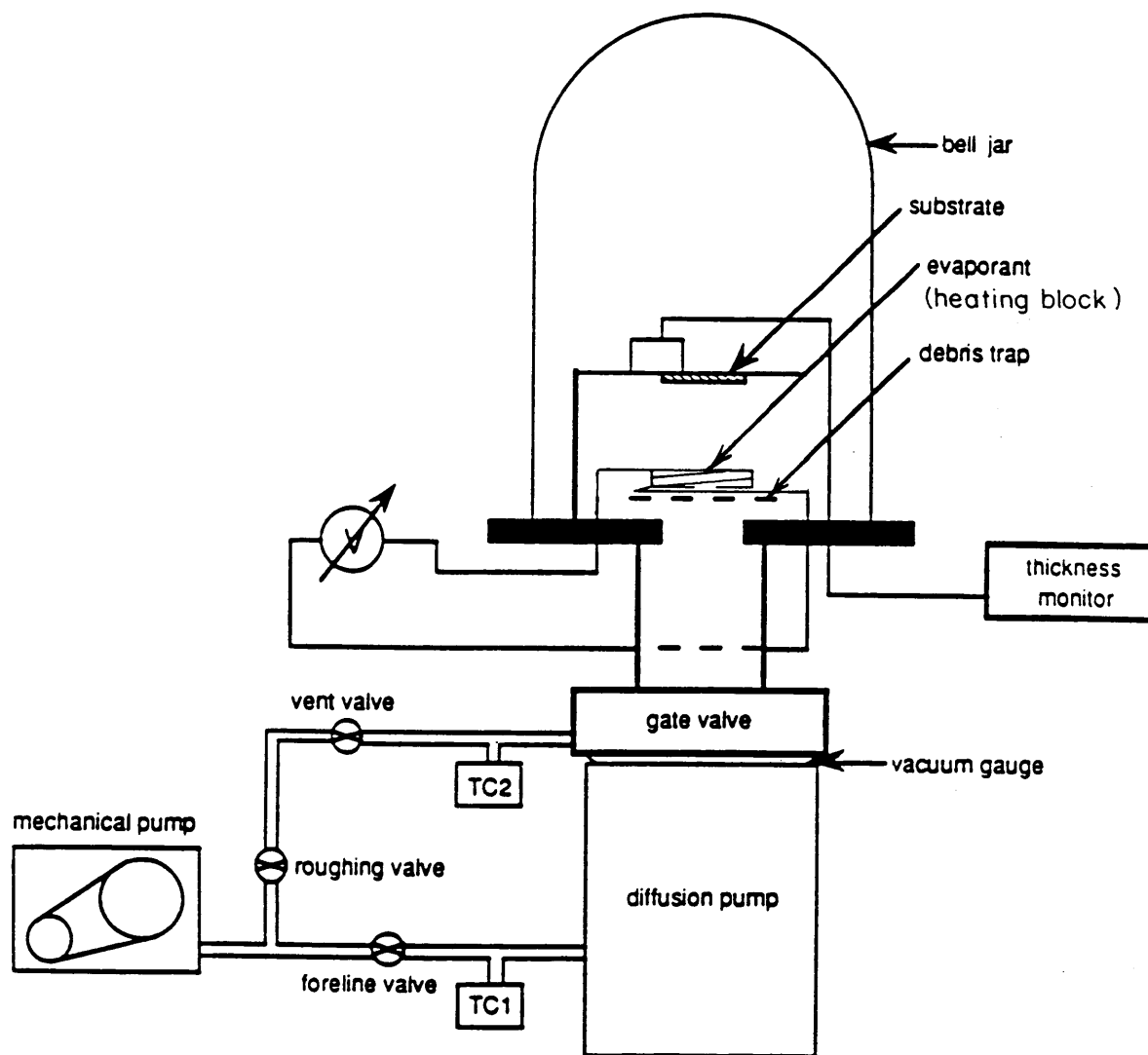


Fig. 1. Apparatus for vacuum-evaporation and film deposition.

It consists of a high vacuum system, a film coating chamber, and a thickness monitor. The temperature was checked by a color scale. The color of the molybdenum heating

wire around the sample heating block determined the temperature at which the sample started to evaporate to within 100°C. The main advantage of preparing the film by vacuum deposition was that the film was protected from contamination, particularly by water. A Veeco/Kronos Model QM311 quartz crystal microbalance was used to monitor the approximate thickness. This allowed us to produce films of optimal thickness for determinations of k in different regions of the spectra. Exact thicknesses were determined after the spectral measurements were completed. The substrates used in this work were sapphire, calcium fluoride, and cesium iodide which are, respectively, transparent over the spectral ranges 0.15–6.5 μm , 0.13–9.0 μm , and 0.30–50 μm . Two substrates and the thickness detector were positioned just above the sample block about 7 cm from the sample, such that the angle of incidence of evaporated sample onto the substrates was close to normal. In all our film depositions, we masked half the area of the substrate with foil in order to measure the transmission through the substrate alone. A thin, even layer of sample around the entire surface of the sample indentation ensured good thermal contact, producing a homogenous beam of evaporated material to be deposited uniformly onto the substrate. Up to 3 depositions were required to produce a sufficiently thick film for optical constants measurements.

The evaporation of kerogen took place in three phases. The rate of deposition was around 10 $\text{\AA} \text{ min}^{-1}$ at the beginning, when the temperature was maintained at roughly 550°C. After about 1 hour the rate of deposition drops rapidly. Raising the temperature to roughly 650°C causes a second, faster phase of deposition which lasts about 30 min. After another drop in rate, the temperature was raised to roughly 750°C, and held there for about 2 hrs., after which no further deposition was noted. The fact that new deposition occurs when the temperature is raised may indicate either the evaporation of different fractions or pyrolytic release of large fragments at higher temperatures. Its color is yellow and during the evaporation, a distinctive odor is noticed. A similar odor was produced while evaporating the Murchison organic extract. After the evaporation, some residues remained in both cases. A total of nine kerogen films were deposited. Three sapphire substrates had film thickness of 0.190, 0.733, and 1.213 μm . Five CsI substrates had films that were 1.089, 1.267, 1.213, 2.100, and 3.000 μm thick, and one CaF_2 substrate had a 0.469 μm thick film.

Similar film preparation methods were repeated to produce films of the Murchison organic residue.

(c) Spectroscopic Measurements

Infrared spectra (2.5–25 μm) of the original, pre-evaporation kerogen and Murchison organic residue samples were obtained with a Nicolet FTIR spectrometer by measuring the transmission through a pellet prepared in a potassium bromide matrix.

1 to 2 mg of material is mixed with about 100 mg of spectrograde KBr powder. After grinding well, the mixed powder is made into a pellet about 0.2 mm thick using a standard dual-bolt pellet press. After removing the bolts, the body of the press is inserted into the beam of the FTIR spectrometer to scan the spectrum.

Transmission spectra (2.5-40 μm) of the vacuum-deposited films on a CsI substrate were obtained at 1 cm^{-1} resolution with a Beckman Acculab Model 10 Infrared spectrometer. Spectra were scanned twice for better accuracy.

A Cary Model 14 PM spectrometer was employed for measurements in the 0.4 to 2.5 μm wavelength region. A Shimadzu spectrometer was employed for measurements from 0.19 to 0.7 μm . We will be using a Seya-Namioka monochromator from 0.13 μm to 0.19 μm in the vacuum UV region for transmission as well as reflection measurements. Reflection measurements from 0.01 μm to 0.17 μm will also be made on a MacPherson Model 247 grazing incidence monochromator.

Imaginary Part of the Refractive Index k

The imaginary part of the refractive index k , is given by Khare et al.¹³ as

$$k = \frac{\lambda}{4\pi t} \ln \frac{T_s (1-R)}{T (1-R_0)^2} \quad (1)$$

where T_s = transmission through substrate

$$R_0 = \left(\frac{n_s - 1}{n_s + 1} \right)^2$$

where n_s = the real part of the refractive index of the substrate, and
 T = transmission through the substrate plus kerogen.

In our case, T_s and T were directly measured and R , the total normal incidence reflectance from the film-substrate system, was estimated by drawing a baseline through the wavelength regions where the film had no significant absorption. If the refractive index, n_f , of the film is determined by an independent method, the equation for R can be computed by

$$R = \frac{(1 + n_f^2)(n_f^2 + n_s^2) - 4n_f^2n_s + (1 - n_f^2)(n_f^2 - n_s^2)\cos \delta}{(1 + n_f^2)(n_f^2 + n_s^2) + 4n_f^2n_s + (1 - n_f^2)(n_f^2 - n_s^2)\cos \delta} \quad (2)$$

$$\text{where, } \delta = \frac{2\pi n_f}{\lambda} (2t) \quad (3)$$

Values of n_s are determined from independent measurement or from the literature.¹⁴ At wavelengths where the real part of the refractive index of the film could not be measured independently, an extrapolated value is used to calculate R for use in Eq. (1).

Real Part of the Refractive Index, n

The real part of the refractive index, n , of kerogen was determined by variable-angle reflectance in the 0.4–2.0 μm wavelength region. To obtain n for a wider wavelength range, we ran a program based on the Kramers-Kronig relation between n and k (Inagaki et al.)¹⁵, given by dispersion relation analysis. When the k values are well determined by transmission measurement, an integral over the energies $E = hc/\lambda$,

$$n(E) - 1 = \frac{2}{\pi} \int_0^{\infty} \frac{E'k(E')}{(E')^2 - E^2} dE' \quad (4)$$

was used to obtain n values. This requires a knowledge of k for high energies (short wavelengths). Since we have not yet determined k on our MacPherson grazing spectrometer that goes down to 0.01 μm , we had to estimate k values for the short wavelength region. We know from past experience that all such organics have a strong feature at $\sim 0.12 \mu\text{m}$. We introduced this feature numerically and adjusted its magnitude such that the Kramers-Kronig analysis on k produced n values consistent with those actually measured at other wavelengths. We will soon measure the k values for kerogen in the short wavelength region to obtain more accurate values of n . Until then the n values outside the range 0.4–2.0 μm should be considered tentative.

RESULTS AND DISCUSSION

(a) FTIR Spectra of Original Pre-Evaporation Samples

The infrared spectra of complex organic solids such as kerogens generally show a limited number of absorption bands which are due to well-defined chemical groups, and can be assigned on the basis of numerous spectra of simple substances.^{5,16,17} The FTIR transmission spectra of the kerogen sample and of the Murchison organic extract are shown in Figure 2. The principle absorption features and their most likely assignments are listed in Table I. The kerogen sample is characterized by strong aromatic absorptions in the 800–1000 cm^{-1} region, and C=O and aliphatic absorptions at 1720 cm^{-1} and 2900 cm^{-1} respectively. It is essentially aromatic in character but has not undergone extensive carbonization as significant amounts of aliphatic and oxygenated material are still present.

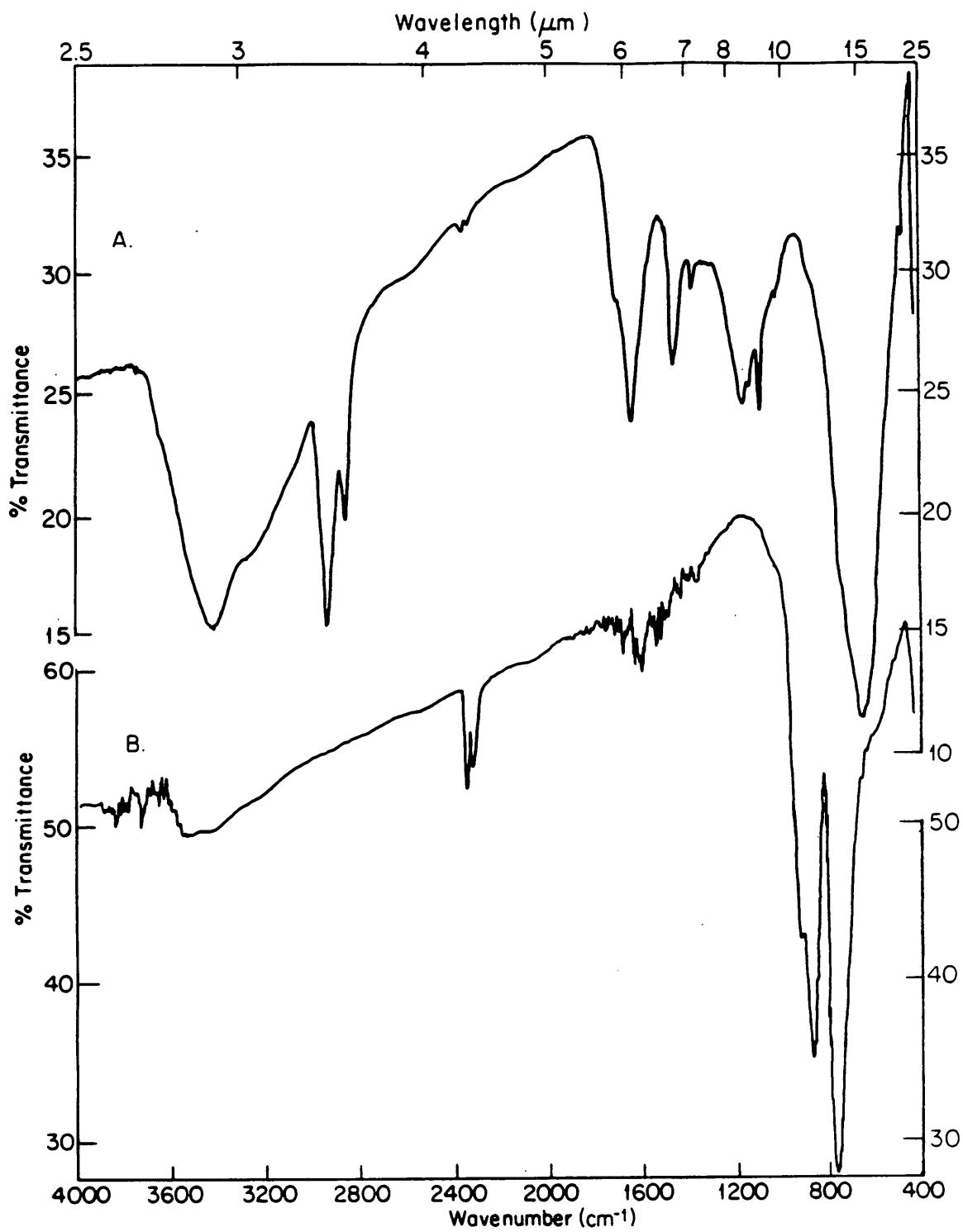


Fig. 2. FTIR transmission spectra in KBr matrix of (A) kerogen Type II (Skye #5) and (B) organic residue from the Murchison meteorite.

Table I

Assignments of absorption features in FTIR spectra of kerogen and organic residue in Murchison meteorite

Wavenumber (cm ⁻¹)	Structural Assignment
3420	OH stretching (absorbed H ₂ O and possible contribution from phenolic, alcoholic, carboxylic OH) ⁴
2924/2853	Alkyl CH stretching
1710 (shoulder)	C=O stretching (minor)
1630	C=C stretching of aromatic and polyaromatic rings (may contain minor C=O stretching)
1455	Asymmetric bending of CH ₂ and CH ₃
870/820/750	Aromatic CH deformation absorptions
650	Out of plane deformation of aromatic CH

The band at 2326 cm⁻¹ is due to atmospheric CO₂ in the spectrometer.

The Murchison organic residue spectrum is clearly dominated by strong aromatic absorptions in the 800-1000 cm⁻¹ region, consistent with existing chemical analysis.^{10,11} No aliphatic absorptions are observed as the corresponding functional groups are apparently contained in relatively soluble components removed by the solvent extraction process. The Murchison "macromolecular" organic material was prepared by HF/HCl dissolution (5 cycles) of ~50 g of freeze/thaw disaggregated bulk meteorite followed by solvent extraction with methanol and toluene to leave a black carbonaceous residue. A similar residue was used by Cruikshank et al.⁷ for reflectance measurements although they incorrectly denoted it as an extract.

(b) FTIR Spectra of Vacuum-Deposited Kerogen

Figure 3 shows the FTIR spectrum of an evaporated film of kerogen deposited on a CsI substrate and the FTIR spectrum of the original kerogen in a KBr matrix for comparison. The strong similarity of the two spectra demonstrates that while the vacuum evaporation process undoubtedly fractionates the kerogen to some degree, the primary functional units are apparently unchanged, and the essential spectral characteristics are preserved. Indeed, the major difference between the two spectra is the near absence of a silicate absorption at around 1200 cm⁻¹ in the evaporated film. The removal of this and other impurities is an incidental benefit of the use of

the thin film vacuum deposition technique for measuring the optical constants of kerogen. The additional detail present in the evaporated film spectrum presumably reflects the higher quality obtainable from optically clear film as opposed to powdered solids.

Figure 4 shows the FTIR spectrum of the residue left after the evaporation. As can be seen, it is essentially featureless, aside from some adsorbed water, some weak

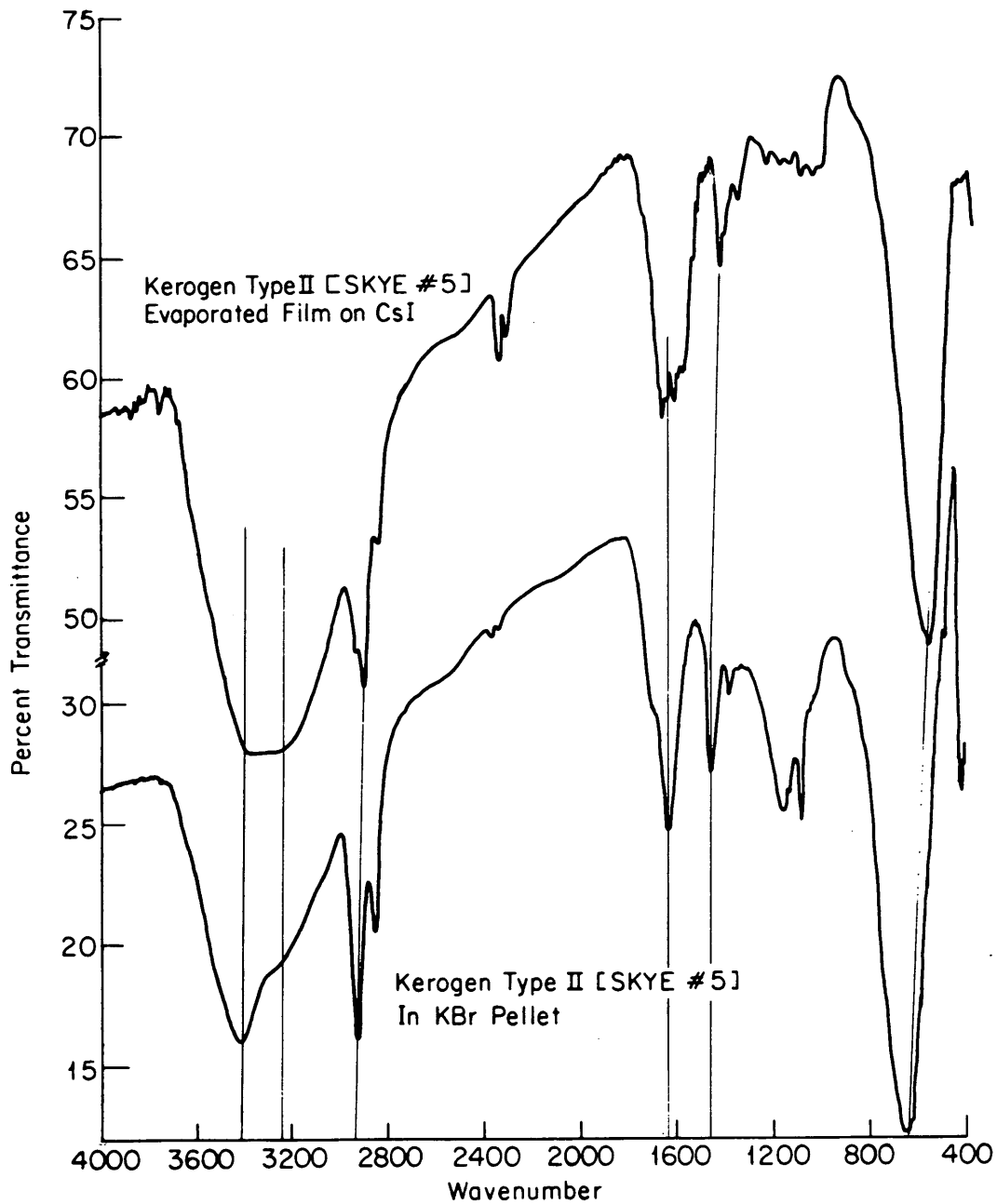


Fig. 3. Vertical lines indicate similarities between the evaporated film of kerogen and the original kerogen in KBr matrix, demonstrating that major spectral features are preserved.

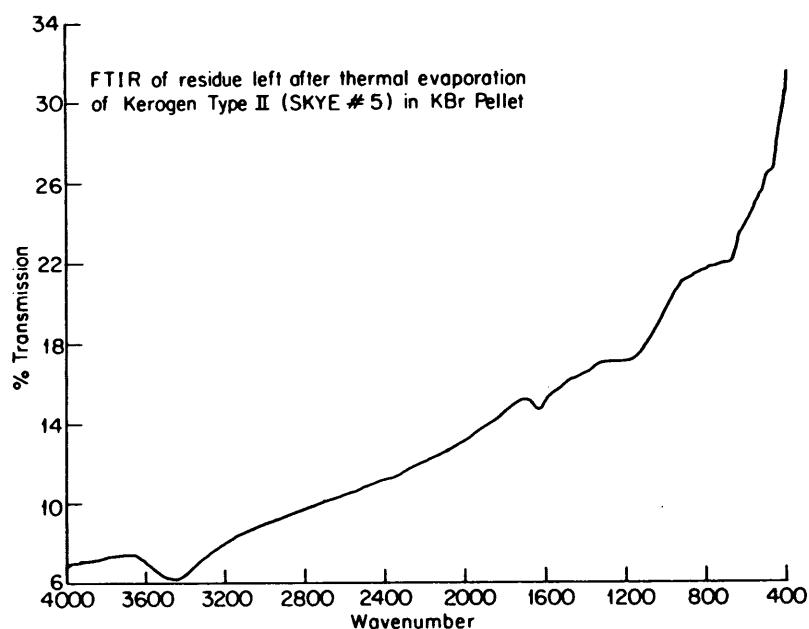


Fig. 4

C-C features, and a slight silicate absorption at 1200 cm^{-1} . Evidently, nearly all of the kerogen is successfully evaporated at 500°C to 750°C .

(c) Infrared Spectra of Films of Murchison Organic Residue and Kerogen

In Figure 5 we show the infrared spectrum of a thermally evaporated film of

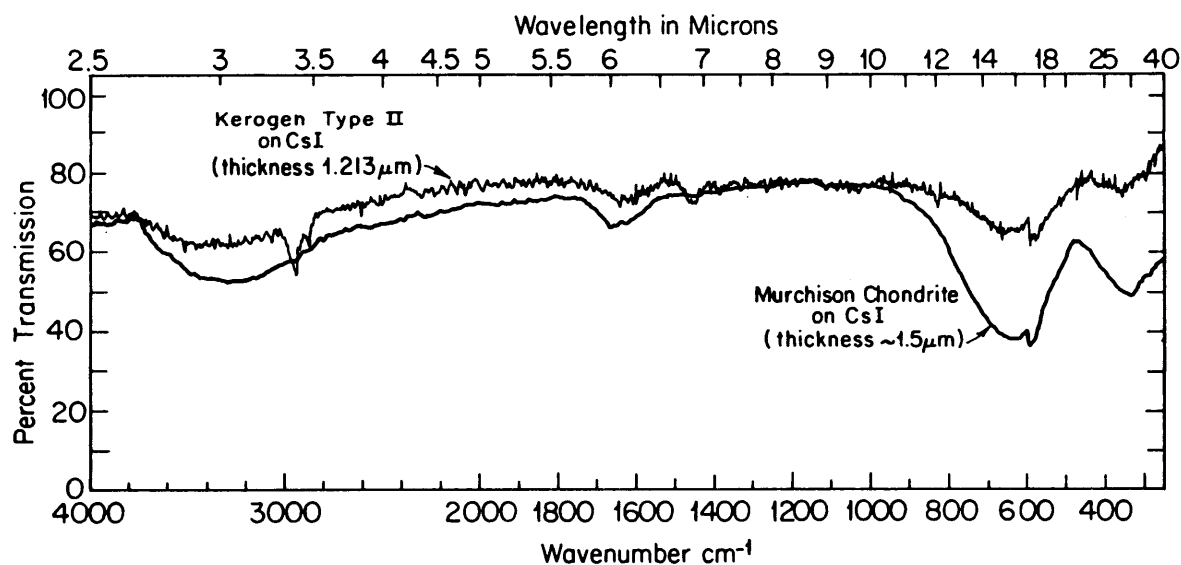


Fig. 5. IR spectra of vacuum-deposited films of Murchison organic residue and Type II kerogen.

Murchison organic residue and compare it with a similarly thermally evaporated film of kerogen. Both of these spectra were obtained with the Beckman Acculab Spectrometer. The films are similar enough in thickness that a direct comparison is possible. The Murchison extract shows spectral features similar to those of the kerogen film, except for the absence of aliphatic CH features near 2900 cm^{-1} and 1450 cm^{-1} . It is significantly more absorbing than the kerogen film we discuss below.

(d) Optical Constants of Kerogen and Meteoritic Organic Material

Using Eq. (1), the spectra, and the measured film thicknesses, the imaginary part of the refractive index, k , was calculated from $0.15\text{-}40\text{ }\mu\text{m}$ for both kerogen and the meteoritic samples. Figure 6 shows results for kerogen graphically; the values

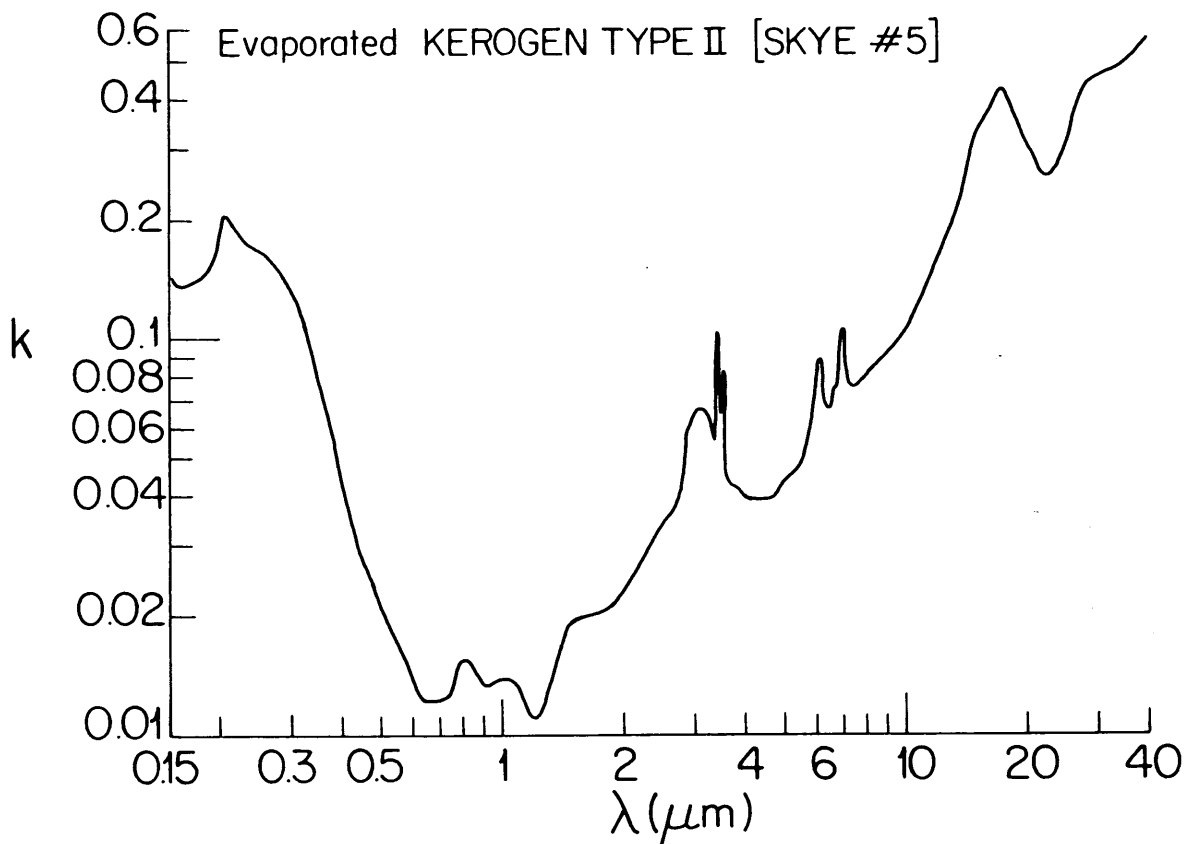


Fig. 6

are also listed in Table II. The values are accurate to $\pm 20\%$ in the UV and IR regions and to $\pm 30\%$ in the visible. Fig. 6 shows that k has substantial structure from $0.15\text{-}40\text{ }\mu\text{m}$.

The real part of the refractive index of kerogen, n , was determined by variable incidence-angle reflectance to be 1.60 ± 0.05 from $0.4\text{ to }2.0\text{ }\mu\text{m}$. Fig. 7 shows the n values computed from k by Kramers-Kronig analysis. The uncertainty is ± 0.05 .

Table II.
Imaginary Part of the Refractive Index (k) = $a10^{-b}$ at Various
Wavelengths (λ) of Thermally Evaporated (to 750°C) Film of Kerogen at Room
Temperature.

λ (μm)	a	b	λ (μm)	a	b	λ (μm)	a	b	λ (μm)	a	b
0.15	1.40	1	0.9	1.33	2	3.356	7.45	2	6.536	6.67	2
0.155	1.35	1	1.0	1.38	2	3.378	8.58	2	6.623	6.76	2
0.16	1.36	1	1.1	1.30	2	3.401	1.02	1	6.667	7.11	2
0.165	1.38	1	1.2	1.10	2	3.425	7.75	2	6.711	7.46	2
0.17	1.39	1	1.3	1.34	2	3.448	6.45	2	6.757	8.00	2
0.1725	1.39	1	1.4	1.75	2	3.472	6.76	2	6.803	9.09	2
0.175	1.40	1	1.5	1.94	2	3.496	8.07	2	6.849	9.50	2
0.18	1.44	1	1.6	1.98	2	3.521	5.13	2	6.897	1.03	2
0.185	1.48	1	1.7	2.03	2	3.546	4.82	2	6.993	9.09	2
0.19	1.56	1	1.8	2.07	2	3.571	4.52	2	7.042	8.50	2
0.195	1.67	1	1.9	2.11	2	3.623	4.49	2	7.143	8.31	2
0.2	1.92	1	2.0	2.27	2	3.650	4.44	2	7.246	8.20	2
0.205	2.01	1	2.1	2.46	2	3.704	4.20	2	7.299	8.00	2
0.21	1.96	1	2.2	2.62	2	3.846	4.05	2	7.407	7.58	2
0.22	1.80	1	2.3	2.92	2	4.	3.97	2	7.692	7.84	2
0.23	1.72	1	2.4	3.02	2	4.167	3.90	2	8.333	8.39	2
0.24	1.69	1	2.5	3.40	2	4.348	3.89	2	9.091	9.40	2
0.25	1.63	1	2.632	3.71	2	4.545	3.92	2	10.	1.01	1
0.28	1.46	1	2.703	3.86	2	4.762	4.01	2	11.111	1.35	1
0.3	1.29	1	2.740	4.39	2	5.	4.36	2	12.5	1.72	1
0.32	1.06	1	2.778	4.93	2	5.128	4.55	2	13.333	2.01	1
0.35	7.72	2	2.817	5.51	2	5.263	4.51	2	14.289	2.71	1
0.38	5.68	2	2.857	5.83	2	5.556	5.16	2	15.384	3.53	1
0.4	4.31	2	2.899	6.02	2	5.714	5.64	2	15.873	4.08	1
0.45	2.84	2	2.941	6.21	2	5.747	5.93	2	16.667	3.84	1
0.5	2.15	2	2.985	6.41	2	5.882	6.91	2	18.182	3.02	1
0.55	1.77	2	3.030	6.62	2	5.952	7.56	2	20.	2.35	1
0.6	1.23	2	3.125	6.42	2	6.061	8.61	2	22.222	2.09	1
0.65	1.23	2	3.226	6.23	2	6.211	8.57	2	25.	2.68	1
0.7	1.23	2	3.289	5.99	2	6.25	8.34	2	28.571	3.86	1
0.75	1.31	2	3.311	5.67	2	6.329	7.87	2	30.303	4.10	1
0.8	1.53	2	3.322	5.54	2	6.41	7.40	2	33.333	3.78	1
0.85	1.46	2	3.333	5.88	2	6.452	7.16	2	40.	2.74	1

k values for the original kerogen can also be estimated from its transmission spectrum in a KBr matrix as shown in Fig. 3. By knowing the percent of kerogen in the KBr pellet and the thickness of the pellet, it was possible to estimate k from 2.5 to 25 μm . Figure 8 compares k of the original material with that obtained for the thin film. (Values are normalized to unity at 16 μm .)

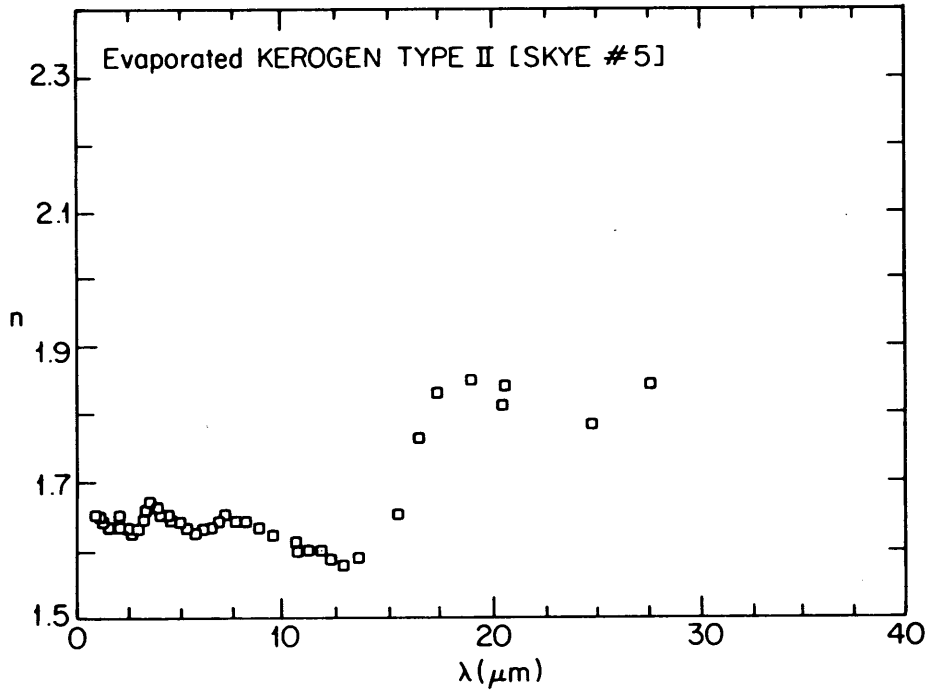


Fig. 7

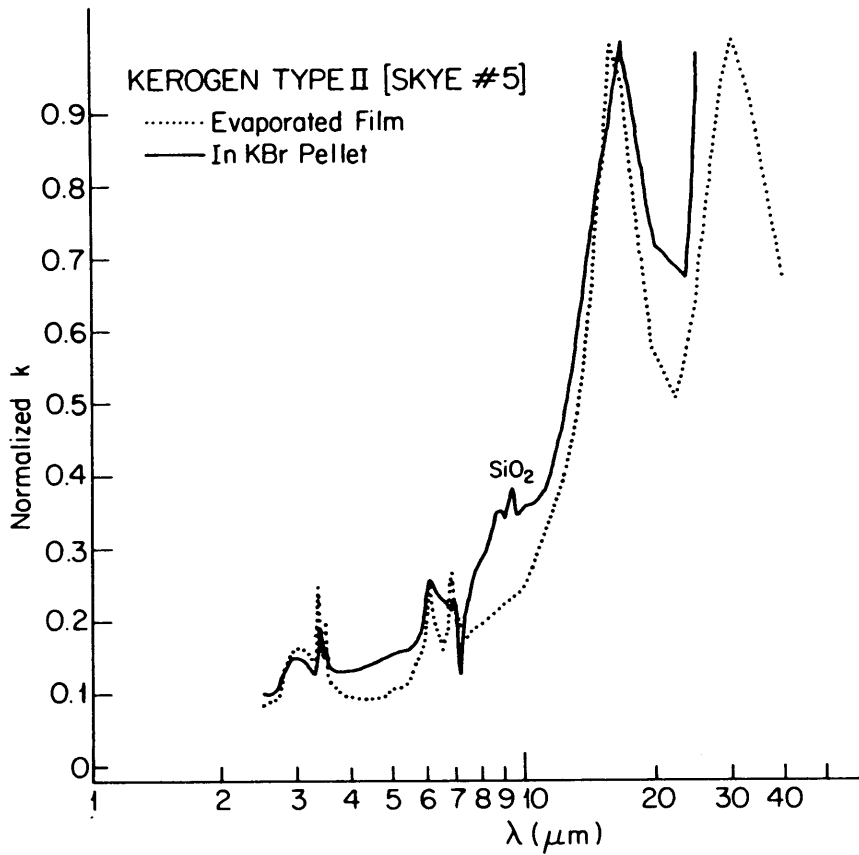


Fig. 8. Comparison of k values for evaporated film of organic matter in Murchison meteorite and evaporated film of kerogen from 2.5 to 40 μm .

The agreement between the normalized k values before and after evaporation is good, again illustrating the preservation of the spectral characteristics of the kerogen after evaporation. As in the FTIR transmission spectra (Fig. 3), the only major differences are due to the lack of silicate absorption in the evaporated film.

Fig. 9 compares the k values obtained for the evaporated kerogen film with the k values of the evaporated Murchison organic residue. Table III lists the k values for the film produced from the Murchison organic extract. The Murchison sample, like Type II kerogen, also shows substantial structure, although k values obtained for Murchison are significantly higher than those of the kerogen, and as expected, do not show any feature associated with aliphatic functional groups.

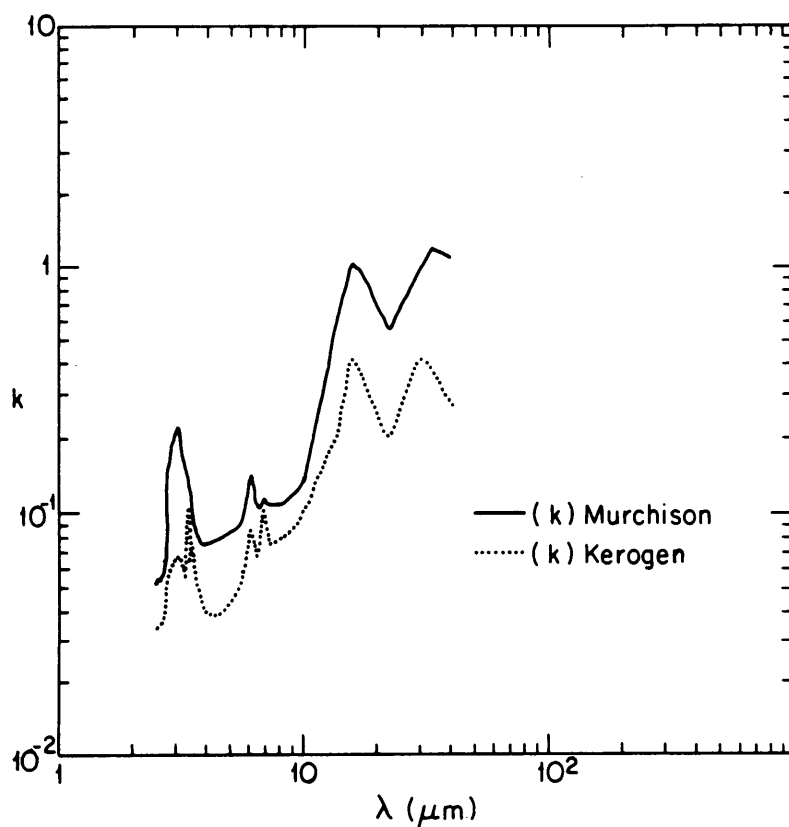


Fig. 9

CONCLUSIONS

(1) The Murchison organic residue has some similarities to Type II kerogen in the infrared, but has a higher k (is more absorbing) and lacks aliphatic spectral features.

Table III.
Imaginary Part of the Refractive Index (k) = $a10^{-b}$ at Various Wavelengths (λ) of Thermally Evaporated (to 750°C) Film of Organics in Murchison Meteorite at Room Temperature.

λ (μm)	a	b	λ (μm)	a	b
2.5	5.28	2	6.25	1.28	1
2.63	5.64	2	6.45	1.09	1
2.70	6.45	2	6.67	1.07	1
2.78	1.09	1	6.89	1.14	1
2.86	1.63	1	7.14	1.09	1
2.94	1.94	1	8.33	1.10	1
3.03	2.16	1	10.00	1.37	1
3.12	1.91	1	11.11	2.25	1
3.23	1.61	1	12.50	3.58	1
3.33	1.40	1	14.29	7.67	1
3.45	1.23	1	15.87	1.02	0
3.57	8.83	2	16.67	9.95	0
3.85	7.55	2	18.18	8.50	0
4.17	7.68	2	20.00	6.96	1
4.55	7.96	2	22.22	5.59	1
5.00	8.35	2	25.00	6.85	1
5.71	9.13	2	28.57	8.90	1
5.88	1.19	1	33.33	1.19	0
6.06	1.41	1	40.00	1.10	0

(2) The thermal evaporation technique is a good method for determining the optical constants of kerogens, organics in meteorites, and probably for other kinds of tholins.⁹

(3) More material is required to produce thick films and pellets to obtain results for the far infrared region to $\lambda = 1$ mm. Transmission measurements in the vacuum UV to soft x-ray region are required to obtain the best determination of n through Kramers-Kronig analysis.

(4) Brooke et al.¹⁸ detect strong 3.4 and 2.8 μm emission features in comet P/Brosen-Metcalf and find that the positions and widths of these features coincide with those observed in comets P/Halley, Wilson (1987 VII), and Bradfield (1987 XXIX). Comets and carbonaceous chondrites probably both accreted from low-temperature condensates in the solar nebula,^{10,19} but the organic residues of comets can derive from pre- and post-accretion irradiation of hydrocarbon-containing ices, a somewhat different origin than that generally envisioned for meteoritic organics.^{8,9} The 3.4 μm CH and 2.8 μm OH features in the above comets well match spectral features found in organic residues of $\text{H}_2\text{O}-\text{CH}_4$ and $\text{H}_2\text{O}-\text{C}_2\text{H}_6$ ice irradiation.^{20,21,22} Similar spectral features in the kerogen suggest not its presence in comets, but simply some basic spectral similarities due to some commonality of functional groups in these materials.

ACKNOWLEDGEMENTS

This research was supported by the Kenneth T. and Eileen L. Norris Foundation, NASA NGR 33-010-101, NSF (EAR-8609218), and NASA (NAG9-52), and by the Office of Health and Environmental Research, U.S. Dept. of Energy under contract DE-AC05-84OR 21400 with Martin Marietta Energy Systems, Inc., ORNL. We appreciate the help of Jonathan Gradie in bringing to our attention some valuable references. We thank Edward Anders for helpful discussions.

REFERENCES

1. B. Durand, Sedimentary organic matter and kerogen. Definition and qualitative importance of kerogen, in *Kerogen, Insoluble Organic Matter from Sedimentary Rocks*, (ed. B. Durand), Editions Technip, Paris, 1980, pp. 13-34.
2. R.D. McIver, Composition of kerogen, Clue to its role in the origin of petroleum. In *Proceedings, 7th World Petroleum Congress*, pp. 25-36.
3. B. Tissot, B. Durand, J. Espitalie, and A. Combaz, *Am. Assoc. of Petroleum Geologist Bull.* **58**, 499 (1974).
4. B.P. Tissot and D.H. Welte, *Petroleum Formation and Occurrence*, Berlin, Springer-Verlag.
5. Robin and Rouxhet, *Geochimica et Cosmochimica Acta* **42**, 1341 (1978).
6. D.P. Cruikshank and R.H. Brown, *Science* **238**, 183 (1987).
7. J.F. Bell, D.P. Cruikshank, and M.H. Goffy, *Icarus* **61**, 192
8. E. Anders, R. Hayatsu, and M.H. Studier, *Science* **182**, 781 (1973).
9. C. Sagan and B.N. Khare, *Nature* **277**, 102 (1979).
10. R. Hayatsu and E. Anders, *Topics of Current Chemistry* **99**, 1-37 (1981), Berlin and Heidelberg: Springer.
11. R. Hayatsu, S. Matsuoka, R.G. Scott, M.H. Studier, and E. Anders, *Geochimica et Cosmochimica Acta* **41**, 1325 (1979).
12. B. Durand and G. Nicaise, Procedures for kerogen isolation, in *Kerogen, Insoluble Organic Matter from Sedimentary Rocks*, (ed. B. Durand), Editions Technip, Paris, 1980, pp. 35-54.
13. B.N. Khare, C. Sagan, E.T. Arakawa, F. Suits, T.A. Callcott, and M.W. Williams, *Icarus* **60**, 127 (1984).
14. G.W.C. Kaye and T.H. Laby, *Tables of Physical and Chemical Constants*, pp. 83-86, Wiley, New York.
15. T. Inagaki, L.C. Emerson, E.T. Arakawa, and M.W. Williams, *Phys. Rev.* **B13**, 2305 (1976).
16. J. Espitalia, B. Durand, J.C. Roussel, and C. Souron, *Rev. de l'Institut Francais de Petrole* **28**, 37 (1973).

17. R.A. Friedel and G.L. Carlson, *Fuel* 51, 194 (1972).
18. T.Y. Brooke, A.T. Tokunaga, J.S. Carr, K. Sellgren, R.F. Knacke, L.J. Allmandola, S.A. Sandford, and M. Tapia, *Bull. Am. Astron. Soc.* 21, 993 (1989).
19. A.H. Delsemme, The origin of comets, in *Comets Asteroids Meteorites -- Interactions, Evolution and Origins*, (ed. A.H. Delsemme), The University of Toledo, 1977, p. 453.
20. C. Chyba and C. Sagan, *Nature* 330, 350 (1987).
21. C.F. Chyba, C. Sagan, and M.J. Mumma, *Icarus* 79, 362 (1989).
22. B.N. Khare, W.R. Thompson, B.G.J.P.T. Murray, C.F. Chyba, and C. Sagan, *Icarus* 79, 351 (1989).